JOURNAL OF SOLID STATE CHEMISTRY 118, 292–298 (1995)

Preparation, Electronic, and Magnetic Properties of $Sr_3V_2O_{6.99}$

J.-G. Lee, K. V. Ramanujachary,[1] and M. Greenblatt

Department of Chemistry, Rutgers, The State University of New Jersey, P.O. Box 939, Piscataway, New Jersey 08855-0939

Received February 17, 1995; in revised form April 27, 1995; accepted April 28, 1995

Synthesis, electrical, and magnetic properties of a layered perovskite-related compound, $Sr_3V_2O_{6.99}$, are reported. Powder X-ray diffraction analysis confirmed the body-centered tetragonal (*I4/mmm*) structure as proposed earlier. The electrical resistivity of the sample is 0.054 Ω·cm at room temperature and decreases with temperature down to 15 K, with a T^2 dependence in the range 15–150 K. The temperature-dependent magnetic susceptibility shows a small cusp at ~110 K. Spin–glass-like behavior is observed in the temperature range 5–26 K as evidenced by irreversibility of the zero-field-cooled and field-cooled magnetization curves. The spin-glass dynamics of the sample was confirmed via the measurement of the AC susceptibility. The observed electrical and magnetic properties suggest disorder-induced localization of the defects at low temperatures.

INTRODUCTION

Since the discovery of high T_c superconductivity in several copper oxide systems, it has been recognized that a systematic study of the highly correlated quasi-two-dimensional oxide systems that exhibit metal-insulator transitions is essential in the formulation of a theoretical basis for the observed high superconducting transition temperatures (1, 2). The reduced binary oxides of vanadium are attractive in this respect since most of them are known to exhibit metal–insulator transitions as a function of the composition and the temperature. In some of the vanadium oxides, such as V_2O_3 and VO_2, etc., the metal–insulator(MI) transitions are accompanied by a modulation of the V–O bond distance (3). Ternary layered perovskites such as Ruddlesden–Popper(RP) phases of the type $Sr_{n+1}V_nO_{3n+1}$ (n = 1 (4–6), 2 (7–10), 3 (11, 12), ∞ (13, 14)) are currently being reexamined by several groups, because of the close resemblance of their structural and anisotropic electronic properties to those of the high T_c copper oxide superconductors (15).

The n = 2 members of RP vanadates, $Sr_3V_2O_{6.8}$ and $Sr_2EuV_2O_{6.8}$, were first prepared by Shin-ike *et al.* in 1976 (7). They indexed the X-ray powder diffraction data on the tetragonal symmetry of $Sr_3Ti_2O_7$ (n = 2 members of RP titanates) and reported the cell parameters a and c, 3.872 and 19.817 Å, respectively, for both compounds. Recently, polycrystalline $Sr_3V_2O_{7-\delta}$, (8–10, 16, 17) as well as single crystals of $Sr_{1.5}La_{1.5}V_2O_7$ (11) have been characterized by several groups. Rieteveld analysis of polycrystalline $Sr_3V_2O_{7-\delta}$ shows a tetragonal structure (*I4/mmm*) with a = 3.8331(7) Å and c = 20.2459(6) Å. However, efforts to increase the charge carrier density by the substitution of La^{3+} for Sr^{2+} and Cr^{3+} for V^{4+} in $Sr_{1.5}La_{1.5}V_2O_7$ and $Sr_3V_{2-x}Cr_xO_7$ (x = 0.0–0.2) have resulted in the disappearance of the metallic property (8, 11). The insulating state of the substituted $Sr_3V_2O_{7-\delta}$ compounds has been attributed to strong electron–electron repulsions resulting in the opening of a Hubbard band-gap near the Fermi level (5, 8, 11). It has been reported that the oxygen deficiency (δ) in polycrystalline $Sr_3V_2O_{7-\delta}$ causes not only a change in the conduction behavior (from metallic to semiconducting at low temperatures), but also anomalous magnetic behavior at 100 K (16). The semiconducting $Sr_3V_2O_{7-\delta}$ ($\delta < 0.12$) also shows irreversibility in the zero-field-cooling (ZFC) and field-cooling (FC) magnetization below about 15 K, reminiscent of a spin–glass-type behavior (10).

In this paper, we report the synthesis of pure polycrystalline $Sr_3V_2O_{7-\delta}$ prepared at a relatively low temperature. The effect of oxygen content on the electrical and magnetic properties is also investigated. The results obtained in this study are compared with those of earlier investigators.

EXPERIMENTAL

SrO (Johnson Matthey, 99.9%), V_2O_5 (Johnson Matthey, 99.9%) and V (Johnson Matthey, 99.5%) were used in the synthesis of $Sr_3V_2O_7$. Single-phase $Sr_3V_2O_7$ was obtained by reducing $Sr_3(VO_4)_2$ with Zr metal in a sealed quartz tube at 1000°C. $Sr_3(VO_4)_2$ was prepared by firing stoichiometric mixtures of SrO and V_2O_5 at 1050°C for 26 hr. Approximately 1.4 g of pelletized $Sr_3(VO_4)_2$ was wrapped in a Zr foil (0.002 × 5.0 × 5.0 cm) and placed in a quartz tube. The Zr foil was used as an oxygen getter

[1] Current address: Rowan College, Glassboro, NJ 08028.

0022-4596/95 $12.00

and as a means of controlling the oxygen pressure (P_{O_2}). The quartz tube was then flushed several times with high purity Ar gas (Matheson, 99.995%) prior to sealing in vacuum ($\sim 10^{-2}$ Torr). The sample in the sealed quartz tube (SQT) was heated in stages: (a) 940°C/12 hr, (b) 980°C/24 hr, and finally (c) 1000°C/18 hr. The heat treatments were interrupted three times for intermediate grinding and repelletization.

The preparation of the solid solution series of the type $Sr_{3-x}Ln_xV_2O_7$ (*Ln* = La and Sm; $0.1 \leq x \leq 0.4$) was attempted using organometallic precursor techniques. Stoichiometric amounts of $Sr(C_2H_3O_2)_2$, $VO(C_5H_7O_2)_2$, $La(C_2H_3O_2)_3 \cdot 1.5H_2O$, and/or Sm_2O_3 were weighed and ground in air. The powdered mixtures were decomposed and calcined at 400 ~ 1100°C in air by increasing the temperature slowly and with intermediate grindings. The resulting white sample was pressed into a pellet and placed in a quartz tube after wrapping in a Zr foil. The quartz tubes were sealed as described above. The sample in the SQT was heated in stages: (a) 950°C/19 hr, (b) 980°C/20 hr, (c) 1000°C/12 hr and finally (d) 1050°C/24 hr.

Products were characterized by a SCINTAG PAD V diffractometer with Cu$K\alpha$ radiation and a liquid N_2 solid state detector. Mica powder (SRM 675 from NBS) was used as an internal standard. Lattice parameters were obtained with a least-squares fitting procedure.

Thermogravimetric analyses (TGA) were performed with a Du Pont 9900 system for the determination of oxygen content. The oxidation state of vanadium was determined by calculating the weight gain on heating up to 900°C and holding for 30 min for the stabilization of the baseline in flowing pure oxygen gas. The oxidized product was assumed to contain only V^{5+}. A heating rate of 5°C/min was used in the TGA measurements.

The d.c. electrical resistivities were measured in a DE 202 cryostat (APD company) by a four-probe method between 15 and 300 K. The sintered pellet was cut into a brick shape ($\sim 0.23 \times 0.42 \times 0.18$ mm) for the measurement. A conducting silver paste and indium metal were used for making four electrical contacts.

Magnetic susceptibility measurements were carried out on brick-shaped pellets with a SQUID magnetometer (Quantum Design) in the temperature range 2–380 K and an applied magnetic field in the range 5–1000 G. The isothermal magnetization data were obtained in the applied magnetic field range 100–2000 G at different temperatures in the range 4–300 K.

Scanning electron micrographs and energy dispersive X-ray spectra were obtained with an Amray 1400 SEM.

RESULTS AND DISCUSSION

Synthetic conditions leading to the formation of a black single-phase $Sr_3V_2O_7$ (Fig. 1) have been optimized by

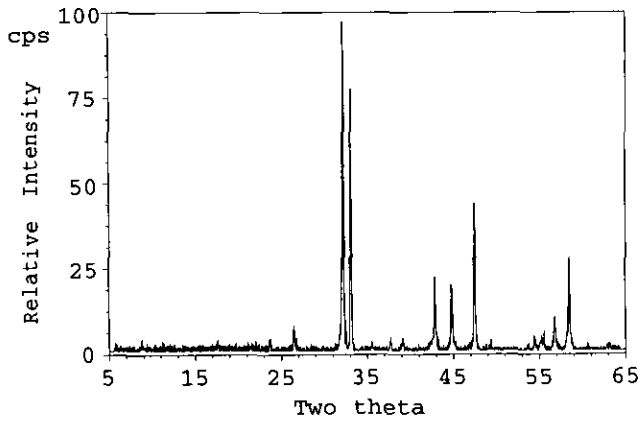

FIG. 1. Powder X-ray diffraction pattern of $Sr_3V_2O_{6.99}$.

varying: (a) the stoichiometry, (b) the reaction atmosphere, and (c) the calcination temperature and heating period. The direct heating of a mixture of SrO, V_2O_5 and V in a ratio of 6 : 1 : 2 in various oxygen-deficient atmospheres at 550~1100°C resulted in a mixture of $Sr_3V_2O_7$, $SrVO_3$, Sr_2VO_4, $Sr_4V_2O_9$ and $Sr_3(VO_4)_2$, etc., as evidenced from the XRD patterns (Table 1). However, the synthesis of pure $Sr_3V_2O_7$ was succesfully accomplished via the precursor method; the pellet (~1.4 g) of the precursor $Sr_3(VO_4)_2$ was wrapped in a Zr foil, placed in a quartz tube, evacuated and heated at 940–1050°C with several intermediate grindings. When the precursor in Zr foil was heated at 1050°C without intermediate grindings in a SQT, it always yielded impure $Sr_3V_2O_7$ with unreacted SrO, Sr_2VO_4, $SrVO_3$, etc. Single-phase $Sr_3V_2O_7$ was prepared only by gradually reducing $Sr_3(VO_4)_2$ wrapped in Zr foil in a sealed quartz tube with several intermediate grindings. The sample prepared was not contaminated by Zr metal as evidenced from energy dispersive X-ray spectra. The lattice parameters, $a = 3.8345(8)$ and $c = 20.259(7)$ Å, were obtained from least-squares fittings of the X-ray diffraction data (Table 2) based on the same space group as that of $Sr_3Ti_2O_7$ (*I*4/*mmm*), and are consistent with previous reports (7–10).

All efforts to substitute Ln^{3+} for Sr^{2+} in $Sr_3V_2O_7$ by solid state methods failed and resulted in multiphases, such as SrO, $SrVO_3$, Sr_2VO_4, $Sr_4V_2O_9$. It is noteworthy that Greedan *et al.* were able to grow $Sr_{1.5}La_{1.5}V_2O_7$ single crystals (11). The $Sr_3V_2O_7$ phase decomposed after extended heating (for example, >2 days) at 1050–1100 K in vacuum. In order to achieve the substitutions, the decomposition of organometallic precursors, $Sr(C_2H_3O_2)_2$, $VO(C_5H_7O_2)_2$, $La(C_2H_3O_2)_2 \cdot 1.5H_2O$, and Sm_2O_3 were tried in the early heating stage and the pellet of the intermediate compounds was reduced in a SQT by Zr metal. We could not prepare pure $Sr_3V_2O_7$ nor substituted $Sr_{3-x}Ln_xV_2O_7$ (*Ln* = La and Sm; $x = 0.0$–0.4) by this

TABLE 1
Results of Various Experimental Conditions in the Synthesis of $Sr_3V_2O_{7-\delta}$

Starting composition	Temp (°C)/ period (hr)[a]	Atmosphere	Phases observed
$3SrO, 2VO_2$	1000/5 ~ 60	Ar	$Sr_3(VO_4)_2(m^+)$
$3SrCO_3, 2NH_4VO_3$	1000/12	Ar	$Sr_3(VO_4)_2(m)$
$3SrO, 2VO_2$	1000/11 ~ 26	SQT[b]	$Sr_3(VO_4)_2(m)$[c]
$3SrO, 2VO_2, 0.5V_2O_3$	1000/11 ~ 26	SQT	$Sr_3(VO_4)_2(m)$[c]
$3SrO, 2VO_2, V_2O_5, V$	1000/11 ~ 26	SQT	$Sr_3(VO_4)_2(m)$[c]
$6SrO, V_2O_5, 2V$	550 ~ 920/14 ~ 24	SQT	$Sr_4V_2O_9(m), Sr_3(VO_4)_2$
$6SrO, V_2O_5, 2V$	900 ~ 1050/10 ~ 72	DV[d]	$Sr_3(VO_4)_2(m), SrVO_3, SrO, Sr_2VO_4$
$6SrO, V_2O_5, 2V$	1050/30 ~ 66	SQT/Zr	$SrVO_3(m), Sr_2VO_4, SrO$, unknown impurity
$6SrO, V_2O_5, 2V$	1050/30 ~ 66	DV/Zr	$SrVO_3, Sr_2VO_4, SrO$, unknown impurity
$Sr_3(VO_4)_2$	940 ~ 1050/24 ~ 96	SQT/Zr	Pure $Sr_3V_2O_7$

[a] With intermediate grindings; m^+, major phase.
[b] Sealed quartz tube.
[c] Sealed quartz tube frequently exploded.
[d] Dynamic vacuum ~5×10^{-4} Torr.

organometallic precursor method. It appears that the thermodynamic stability of $Sr_3V_2O_7$ is in a very narrow range of oxygen partial pressure and temperature.

TGA measurements were performed on the powdered samples to determine the oxygen content in $Sr_3V_2O_{7-\delta}$. The average δ value is calculated to be 0.01 ± 0.01 based on the weight gain after complete oxidation to V^{5+} in flowing oxygen atmosphere (holding for 30 min at 900°C).

The temperature dependence of the electrical resistivity of $Sr_3V_2O_{6.99}$ is shown in Fig. 2. The resistivity decreases linearly with decreasing temperature from $\rho_{RT} = 0.054\ \Omega \cdot cm$ to $\rho_{15\,K} = 0.024\ \Omega \cdot cm$; below ~160 K, the temperature dependence of resistivity shows deviation from linearity. The low temperature resistivity values below ~160 K could be fitted well to the relationship: $\rho(T) = \rho(0) + AT^2$ (13, 18). This T^2 behavior at low temperatures might be attributed to either electron–electron scattering arising from V^{3+} centers created by the oxygen defects, or the presence of electrons in narrow bands, thus increasing their effective mass. Both effects are observed in disordered metals and are considered to be extrinsic effects (13, 18). Indeed, oxygen defects were observed in $Sr_3V_2O_{7-\delta}$, with $-0.01 \leq \delta \leq 0.31$ as shown in Table 3, depending on the synthetic heating history (7–10). Oxygen deficiencies also have been observed in the other members of RP vanadates, for example $SrVO_{3-\delta}$ ($\delta = -0.125 \sim 0.5$) (13, 14), $Sr_4V_3O_{10-\delta}$ ($\delta = 0.10 \sim 0.59$) (11, 12) and $Sr_2VO_{4-\delta}$ ($\delta = \sim 0.01$) (5–7, 19). Thus, when δ is 0.31, the formal charge can be assigned as $Sr_3^{2+}V_{1.38}^{4+}V_{0.62}^{3+}O_{6.69}$ and the electron–electron correlations arising from V^{3+} are expected to be significant. On the other hand, the room temperature resistivity values as a function of oxygen

TABLE 2
Powder X-Ray Diffraction Data of $Sr_3V_2O_7$ Phase, Space Group *I4/mmm*

hkl	d_{obs} (Å)	d_{calc} (Å)	I/I_0
101	3.78	3.77	5
006	3.38	3.38	9
105	2.786	2.785	99
110	2.713	2.711	75
114	2.391	2.390	4
107	2.309	2.310	4
116	2.114	2.114	19
00, 10	2.025	2.026	21
200	1.916	1.917	36
11, 10	1.623	1.623	9
215	1.580	1.580	23

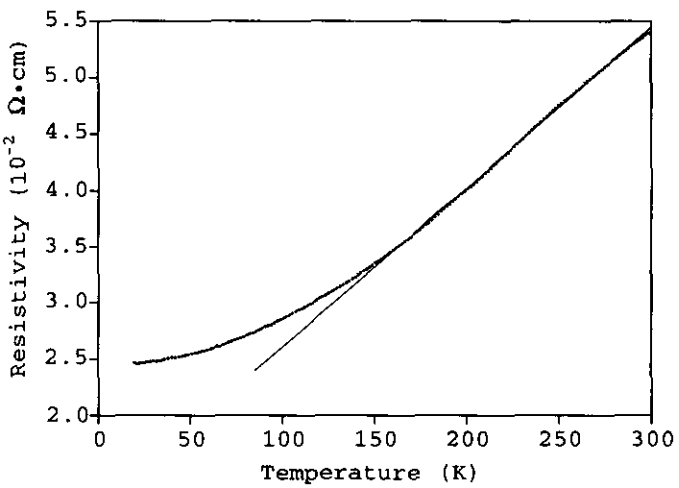

FIG. 2. Electrical resistivity of $Sr_3V_2O_{6.99}$ in the range 15–300 K.

TABLE 3
Resistivity and Unit Cell Parameters of $Sr_3V_2O_{7-\delta}$ at Room Temperature

δ	ρ ($\Omega \cdot$ cm)	a (Å)	c (Å)	Reference
−0.01	0.0048	3.8331(7)	20.2459(6)	N. Suzuki[a]
0.01	0.054	3.8345(8)	20.259(7)	This work
0.06	0.05	3.839(1)	20.25(1)	A. Nozaki[a]
0.12[b]	0.02	3.8399(1)	20.237(1)	M. Itoh
0.27[b]	0.09	[c]	[c]	H. Niu
0.31[b]	0.07	[c]	[c]	H. Niu

[a] Determined from Rietveld analysis.
[b] Resistivity at low temperatures is higher than ρ_{RT} and the samples show spin freezing behavior at low temperatures.
[c] Not reported.

deficiencies in $Sr_3V_2O_{7-\delta}$ shown in Table 3 more or less increase with increasing δ (oxygen deficiency). Furthermore, for samples with higher oxygen deficiency ($\delta > 0.12$), semiconducting behavior is observed at low temperature (i.e.,there is a metal–insulator transition).

The magnetic susceptibility of $Sr_3V_2O_{6.99}$ as a function of temperature is shown in Fig. 3. Both Pauli paramagnetic and Curie–Weiss-like behavior are observed to coexist in the sample. Therefore, the total susceptibility, $\chi(T)$, for $Sr_3V_2O_{6.99}$ is analyzed as the sum of temperature-independent (χ_0), diamagnetic (χ_{dia}), and Curie–Weiss ($\chi_c(T)$) terms,

$$\chi(T) = \chi_0 + \chi_{dia} + \chi_c(T), \quad \text{where } \chi_c(T) = C/(T - \theta). \quad [1]$$

The susceptibility χ_{dia} resulting from the ion cores was negligible (calculated to be $\sim -1.4 \times 10^{-4}$ emu/mol) and

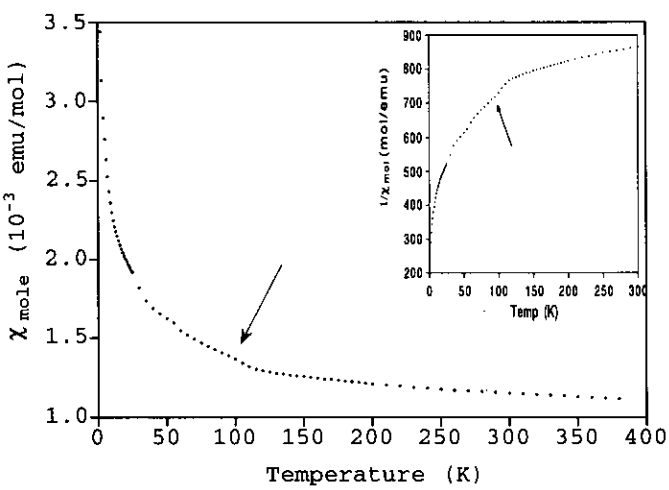

FIG. 3. Temperature-dependent magnetic susceptibility of $Sr_3V_2O_{6.99}$ at an applied field ~1000 G. The $1/\chi$ vs. T plot is shown in the inset.

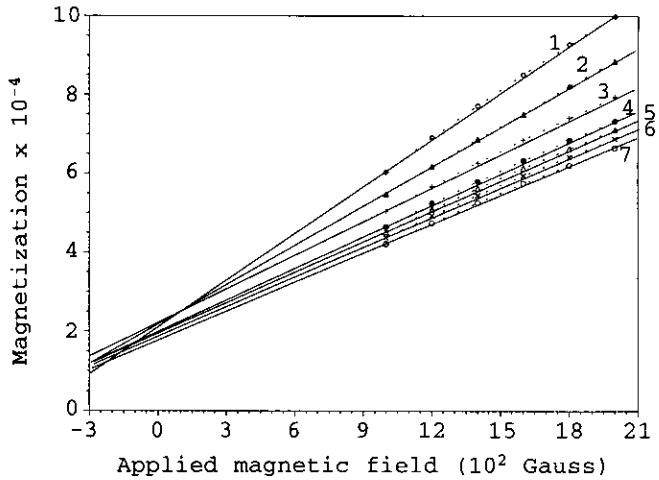

FIG. 4. Magnetization measurement of $Sr_3V_2O_{6.99}$ as a function of applied magnetic field 100–2000 G in the range 30–300 K. Curves 1–7 are obtained from the measurements at 30, 60, 90, 120, 150, 200, and 300 K, respectively.

hence was not considered. A kink in the magnetization data at ~110 K is evident upon close inspection of Fig. 3 (see the arrow). This small anomaly, also noted by Nozaki and co-workers (16), can be explained in terms of a small canting of the antiferromagnetically ordered magnetic moments of $V^{4+}(3d^1, S = 1/2)$. In order to further verify this phenomenon, we have carried out detailed isothermal magnetization studies and the results are shown in Fig. 4. It is evident from Fig. 4 that below 100 K, the isotherms intersect at ~110 G, presenting strong evidence for the existence of remanent magnetization. Above 100 K, however, the field-dependent magnetization isotherms are parallel to each other, implying the absence of remanent magnetization. These results suggest that the V^{4+}–O^{2-}–V^{4+} antiferromagnetic exchange symmetry breaks down below ~100 K, leading to weak ferromagnetism. The canting behavior in $Sr_3V_2O_{7-\delta}$ may be related to a minor structural distortion, which removes the symmetry of spin pairs, required by the Dzyaloshinsky–Moriya model (20). Similar behavior has also been observed in several layered cuprates with orthorhombic symmetry. Detailed magnetic studies on oriented single crystals would be necessary for the characterization of the anomalous magnetic behavior observed in layered RP vanadates. In particular, neutron diffraction studies determining the precise spin orientation of the ordered state are also called for. The experimental magnetic parameters, χ_o, C, and θ are also comparable to those reported previously and are presented in Table 4. The high χ_o value may be attributed to the high density of states in a narrow conduction band at the Fermi level, according to the equation (21):

TABLE 4
Magnetic Constants of $Sr_3V_2O_{7-\delta}$

Composition	χ_0[a]	C[b]	μ_B[d]	θ[c]	Reference
$Sr_3V_2O_{6.94}$	6.67×10^{-4}	0.373	0.4	24	A. Nozaki
$Sr_3V_2O_{6.88}$	4.50×10^{-4}	0.036	0.38	37	M. Itoh
$Sr_3V_2O_{7.01}$	5.40×10^{-4}	0.034	0.37	−1.6	N.Suzuki
$Sr_3V_2O_{6.99}$	10.4×10^{-4}	0.0325	0.36	9.9	This work

[a] Temperature-independent susceptibility (emu/mole).
[b] Curie constant (K · emu/mole).
[c] Weiss constant (K).
[d] Effective magnetic moment per V ion.

$$\chi = \mu^2 D(E_f) \quad [2]$$

μ = magnetic moment

$D(E_f)$ = density of states at Fermi level = $3N/2E_f$

N = the total number of orbitals (conduction electrons)

E_f = energy at the Fermi level.

For a more accurate estimation of χ_0 and C, the magnetic susceptibility data were analyzed in terms of $\chi \cdot T$ vs T. As shown in Fig. 5, the $\chi \cdot T$ data fit to a straight line down to ~80 K, and χ_0 and C can be calculated based on the equation:

$$\chi(T) = \chi_0 + C/(T - \theta). \quad [3]$$

If both sides of Eq. (3) are multiplied by T, and θ is very small,

$$\chi \cdot T = \chi_0 \cdot T + C. \quad [4]$$

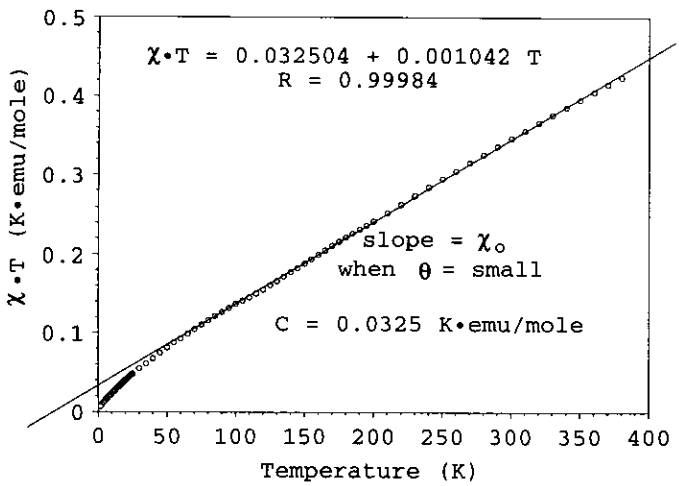

FIG. 5. $\chi \cdot T$ vs T plot of $Sr_3V_2O_{6.99}$ at applied magnetic field 1000 G in the range 2–400 K.

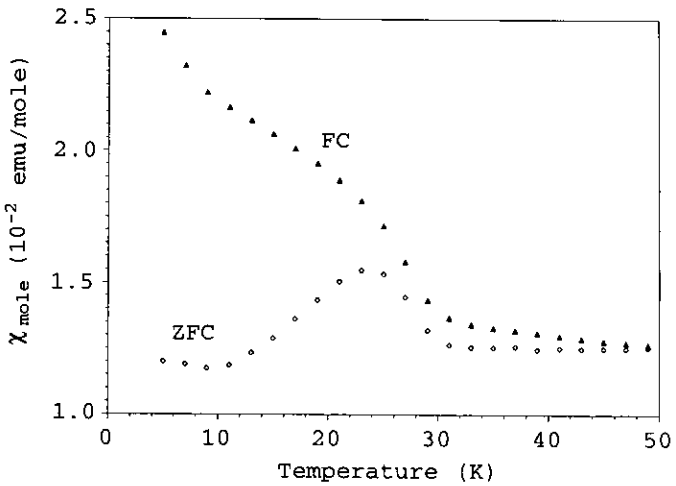

FIG. 6. Spin freezing behavior of $Sr_3V_2O_{6.99}$ observed at low applied magnetic field, 10 G.

Below ~80 K, the data merged to zero. For the straight line in Fig. 5, the fit to Eq. [4] is $\chi \cdot T = 0.0325 + 0.00104T$, the slope χ_0 and the intercept C are 0.00104 emu/mole and 0.0325 K · emu/mole, respectively.

The temperature-dependent magnetic susceptibility measured under field-cooled (FC) and zero-field-cooled (ZFC) conditions at an applied field of 10 G for $Sr_3V_2O_{6.99}$ is illustrated in Fig. 6. A dramatic difference between ZFC and FC data are observed at low temperature. The cusp-like feature at ~24 K in ZFC data indicates the onset of a spin–glass-like transition. The spin–glass temperature observed in the sample is higher than those reported in $Sr_3V_2O_{7-\delta}$ (~15 K) (10) and in VO_x(<10 K) (22). However, we note that the relatively high spin–glass temperature of a freshly prepared $Sr_3V_2O_{6.99}$ decreased to lower temperatures (5–7 K) and finaly disappeared after the sample was kept in air for 1–2 years.

In order to investigate the origin of the anomalous behavior of spin–glass transition in $Sr_3V_2O_{7-\delta}$, polycrystalline samples were prepared in sealed quartz ampoules in two different ways; some samples were outgassed at ~10^{-2} Torr, while other batches of samples were prepared at ~10^{-6} Torr. Single-phase $Sr_3V_2O_{7-\delta}$ could be obtained at the low vacuum (~10^{-2} Torr) condition by heating the sample for ~1.8 days or less at 960–1030°C with intermittant regrindings and repelletizations as described before. However, the high-vacuum (~10^{-6} Torr) preparations required slightly higher and/or much longer heat treatment (<~3.5 days) for the formation of single-phase $Sr_3V_2O_{7-\delta}$. Although the samples preapared under these different vacuum conditions had identical X-ray patterns, and were both metallic, their magnetic behavior was dramatically different. Samples prepared under high vaccum (~10^{-6} Torr) did not show any evidence of spin–glass transition

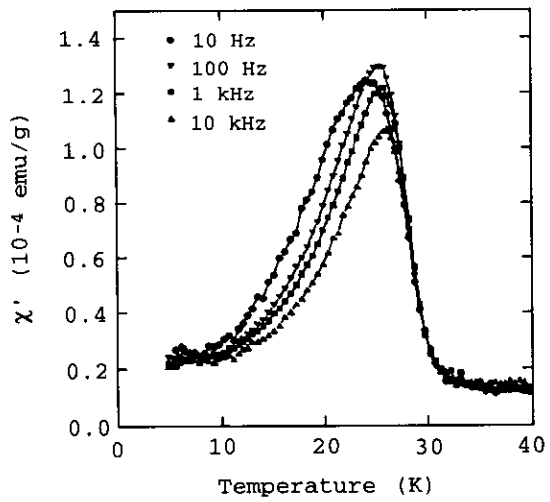

FIG. 7. The real susceptibility component, χ' of $Sr_3V_2O_{6.95}$ as a function of temperature at different frequencies, 10, 100, 1000, and 10000 Hz. The lower susceptibility values at T_f for 10 Hz data are due to the higher field amplitude employed in the measurement.

down to 6 K, although a weak signature was observed below 6 K in some samples. On the other hand, samples prepared under lower-vacuum conditons ($\sim 10^{-2}$ Torr) revealed the divergence of the ZFC and FC magnetization curves, indicating spin–glass transition at $T_f = \sim 24$ K.

We have measured the oxygen deficiency (δ) in $Sr_3V_2O_{7-\delta}$ prepared under different vacuum conditions and found the value of δ to be the same ($\sim 0.05 \pm 0.01$) regardless of the residual pressure of the tubes. Thus the apparent differences in the magnetic properties may be related to subtle changes in the ordering of vacancies, rather than the total oxygen content of the samples. Thus, one can argue that the samples prepared at $\sim 10^{-2}$ Torr are more disordered in terms of the oxygen vacancies than samples prepared at $\sim 10^{-6}$ Torr (i.e., they needed longer heating and/or slightly higher temperatures), which is consistent with the observation of spin–glass transition in the more disordered $Sr_3V_2O_{7-\delta}$ sample (10).

In order to unambiguously confirm the spin–glass transition observed in $Sr_3V_2O_{7-\delta}$ ($\delta = 0.05 \pm 0.01$), temperature-dependent AC susceptibility was measured in zero DC bias field at $H_{ac} = 1$ Oe at different frequencies, 10, 100, 1000, and 10000 Hz. The AC susceptibility is considered as the sum of both real and imaginary susceptibilities,

$$\chi_{ac} = \chi(\omega, T) = \chi'(\omega, T) + i\chi''(\omega, T), \qquad [5]$$

where χ' and χ'' are the real and imaginary susceptibilities, respectively. The frequency dependence of the cusp-like feature observed in the real and imaginary susceptibilities is consistent with the characteristics of spin–glass transition, i.e., T_f increases with increasing frequency as shown in Fig. 7, $T_f = 24.3$, 25.3, 25.6, and 26.1 K for the frequencies 10, 100, 1000, and 10000 Hz, respectively.

The origin of spin freezing in $Sr_3V_2O_{7-\delta}$ was explained by Niu *et al.* in terms of localized vanadium spins (V^{3+}, d^2 ions) interacting via the conduction electrons (10). The mechanism of this exchange interaction was suggested to be a Rudermann–Kittel–Kasuya–Yoshida (RKKY) type (10). The samples of Niu *et al.* were semiconducting and had δ values on the order of ~ 0.30 and the spin–glass behavior was attributed to the disordering of the oxygen vacancies. Although δ is much smaller in our samples (~ 0.01–0.05), our samples are metallic, hence the RKKY mechanism facilitating the spin–glass transition is helped by the larger concentration of conduction electrons. Finally, the disappearance of the spin–glass behavior ($T_f \approx$ 24 K) in the aged samples can be understood in terms of the partial oxidation of V^{3+} to V^{4+} in air after a period of 1–2 years. However, oxidation would decrease the value of δ as well.

CONCLUSIONS

Single-phase polycrystalline $Sr_3V_2O_{7-\delta}$ ($\delta = \sim 0.01$–0.05) was prepared for the first time by reducing $Sr_3(VO_4)_2$ with Zr metal, which controlled the partial pressure of oxygen. Powder X-ray diffraction analysis confirmed the body-centered tetragonal (*I4/mmm*) structure as proposed earlier. Resistivity data was observed to follow a T^2 behavior below 160 K, while oxygen-deficient phases ($\delta \geq 0.27$) prepared by others exhibit a broad metal–insulator transition below ~ 100 K. In contrast to previous results, where spin–glass behavior was observed at ~ 15 K in a highly oxygen deficient ($\delta \approx 0.30$) and semiconducting $Sr_3V_2O_{7-\delta}$ phase (10), we observe spin–glass-like behavior at $T_f = 24$ K in metallic $Sr_3V_2O_{7-\delta}$ with very small values of δ ($\delta = 0.01$–0.05) and only in samples prepared at moderately low oxygen pressures ($P = \sim 10^{-2}$ Torr). The spin–glass transition was confirmed by AC susceptibility measurements, which show that T_f increases from 24.3 to 26.1 K with a frequency increase from 10 to 10000 Hz. A spin canting behavior at ~ 110 K was evident from the magnetization measurements.

ACKNOWLEDGMENTS

We thank B. C. Dodrill of Lake Shore Cryotronic, Inc. for the measurement of AC susceptibility data on a Lake Shore Series-7000 Susceptometer/Magnetometer. We thank Professor Bill McCarroll for critically reading this manuscript. This work was supported by NSF Solid State Chemistry Grants DMR-91-19301 and DMR-93-14605.

REFERENCES

1. J. Bardeen, L. N. Cooper, and J. R. Schrieffer, *Phys. Rev.* **106,** 162 (1957).
2. "High Temperature Superconductors: Relationships Between Properties, Structure, and Solid-State Chemistry", *in Mat. Res. Soc.*

Symp. Proc. 1989; A. Nalikar, "Studies of High Temperature Superconductors," Vol. 1–6. Nova Science Publishers, New York, 1992.
3. J. B. Goodenough, *J. Solid State Chem.* **3,** 490 (1971); D. B. Rogers, R. D. Shannon, A. W. Sleight, and J. L. Gillson, *Inorg. Chem.* **8,** 841 (1969).
4. R. J. D. Tilley, *J. Solid State Chem.* **21,** 293 (1977); R. Scholder and W. Klemm, *Angew. Chem.* **66**(16), 461 (1954).
5. W. E. Pickett, D. Singh, D. A. Papaconstantopoulos, H. Krakauer, M. Cyrot, and F. Cyrot-Lackmann, *Physica C* **162–164,** 1433 (1989).
6. V. A. Fotiev and G. V. Bazuev, *Russ. J. Inorg. Chem.* **26**(4), 474 (1981); A. Feltz and S. Schmalfus, *Z. Chem.* **15,** 289 (1975); M. J. Rey, P. Dehaudt, J. C. Joubert, B. Lambert-Andron, M. Cyrot, and F. Cyrot-Lackmann, *J. Solid State Chem.* **86,** 101 (1990); M. Cyrot, B. Lambert-Andron, J. L. Soubeyroux, M. J. Rey, P. Dehauht, F. Cyrot-Lackmann, G. Fourcaudot, J. Beille, and J. L. Tholence, *J. Solid State Chem.* **85,** 321 (1990).
7. T. Shin-ike, T. Sakai, G. Adachi, and J. Shiokawa, *Mat. Res. Bull.* **11,** 801 (1976).
8. N. Fukushima, S. Tanaka, H. Niu, and H. Ando, *Jpn. J. Appl. Phys.* **29**(12), L2190 (1990).
9. N. Suzuki, T. Noritake, N. Yamamoto, and T. Hioki, *Mat. Res. Bull.* **26,** 1 (1991).
10. H. Niu, N. Fukushima, and K. Ando, *Phys. Rev. B* **44**(9), 4724 (1991).
11. W. Gong, J. S. Xue, and J. E. Greedan, *J. Solid State Chem.* **91,** 180 (1991).
12. M. Itoh, M. Shikano, R. Liang, H. Kawaji, and T. Nakamura, *J. Solid State Chem.* **88,** 597 (1990); N. Suzuki, T. Noritake, N. Yamamoto, and T. Hioki, *Mat. Res. Bull.* **26,** 75 (1991); S. Takeno, S.-I. Nakamura, T. Nomaki, N. Fukushima, and K. Ando, *J. Solid State Chem.* **94,** 432 (1991); N. Ohashi, Y. Teramoto, H. Ikawa, and O. Fukunaga, *J. Solid State Chem.* **97,** 434 (1992).
13. M. Onoda, H. Ohta, and H. Nagasawa, *Solid State Commun.* **79**(4), 281 (1991).
14. B. L. Chamberland and P. S. Danielson, *J. Solid State Chem.* **3,** 243 (1971); P. Dougier, J. C. C. Fan, and J. B. Goodenough, *J. Solid State Chem.* **14,** 247 (1975); T. Palanisamy, J. Gopalakrishnan, and M. V. C. Sastri, *Z. Anorg. Allg. Chem.* **415,** 275 (1975); A. K. Shulka and A. Gupta, *Indian J. Phys.* **53A,** 299 (1979).
15. S. N. Ruddlesden and P. Popper, *Acta Crystallogr.* **10,** 538 (1957); M. Itoh, M. Shikano, H. Kawaji, and T. Nakamura, *Solid State Commun.* **80**(8), 545 (1991).
16. A. Nozaki, H. Yoshikawa, T. Wada, H. Yamauchi, and S. Tanaka, *Phys. Rev. B* **43**(1), 181 (1991).
17. S. Takeno, S.-i. Nakamura, N. Fukushima, and K. Ando, *J. Alloys Comp.* **187,** 31–37 (1992).
18. M. Gurvitch, A. K. Ghosh, H. Lutz, and M. Strongin, *Phys. Rev. B* **22**(1), 128 (1980).
19. J. M. Longo and P. M. Raccah, *J. Solid State Chem.* **6,** 526 (1973); T. Shin-ike, T. Sakai, and J. Shiokawa, *Mater. Res. Bull.* **12,** 831 (1977); F. Deslandes, A. I. Nazzal, and J. B. Torrance, "Research Report, Solid State Physics," RJ 8103 (74042), May 7, 1991; J. E. Greedan and W. Gong, *J. Alloys Comp.* **180,** 281 (1992).
20. I. Dzyaloshinsky, *J. Phys. Chem. Solids* **4,** 241 (1958); T. Moriya, *Phys. Rev.* **120**(1), 91 (1960); S.-W. Cheong, J. D. Thompson, and Z. Fisk, *Phys. Rev. B* **39**(7), 4395–4398 (1989); S.-W. Cheong, J. D. Thompson, and Z. Fisk, *Physica C* **158,** 109–126 (1989).
21. C. Kittel, "Introduction to Solid State Physics," 6th ed. Wiley, New York, 1971.
22. T. Ohtani, K. Kosuge, and S. Kachi, *Solid State Commun.* **36,** 575 (1980); V. Cannella and J.A. Mydosh, *Phys. Rev. B* **6**(11), 4220 (1972).